Analysis of the un-stressed lattice spacing, d_0, for the determination of the residual stress in a friction stir welded plate of an age hardening aluminum alloy – Use of equilibrium conditions and a genetic algorithm

F. Cioffi[1], J.I. Hidalgo[2], R. Fernández[1], T. Pirling[3], B. Fernández[1], D. Gesto[4], I. Puente Orench[3], P.Rey[4], G. González-Doncel[1*]

(1) Dept. of Physical Metallurgy, Centro Nacional de Investigaciones Metalúrgicas, CENIM, C.S.I.C., Av. de Gregorio del Amo 8, 28040 Madrid, Spain

(2) Dept. de Arquitectura de Computadores y Automática, Universidad Complutense de Madrid, 28040 Madrid, Spain

(3) Diffraction Group, Institut Laue-Langevin, ILL, BP156, F-38042, Grenoble Cedex 9, France

(4) Centro Tecnológico AIMEN, C. Relva 27, E-36410,O Porriño. Spain

Abstract

Procedures based on equilibrium conditions (stress and bending moment) have been used to obtain an un-stressed lattice spacing, d_0, as a crucial requirement for calculating the residual stress, RS, profile across a joint conducted on a 10 mm thick plate of AA2024 alloy by friction stir welding, FSW. Two procedures have been used. First, equilibrium conditions were imposed on sections parallel to the weld so that a constant d_0 value corresponding to the base material region could be calculated analytically. Second, balance conditions were imposed on a section transverse to the weld. Then, making use of the neutron diffraction measurements and a genetic algorithm, suitable d_0 values for the different regions of the weld have been found. The RS profile calculated by these two methods were compared and discussed ~~together with the results derived from measurements conducted on a comb sample.~~ For several reasons, the comb method proves to be inappropriate for RS determination in this case. The equilibrium conditions, together with the genetic algorithm, however, has shown to be very suitable to determine RS profiles in FSW of age hardening alloys, where inherent microstructural variations of d_0 across the weld are expected. (193)

Key words

Residual stress; Genetic Algorithms; Neutron diffraction; Aluminum alloys; Friction stir welding, FSW.

*Corresponding author; ggd@cenim.csic.es, tel. +34 91 5538900, ext. 337

1.- Introduction

Probably, the most critical issue for the determination of the residual stress, RS, state of a given sample/component by diffraction methods (usually x-rays or neutrons) is the availability of an accurate and reliable value of the un-stressed lattice spacing, d_0 [1,2,3,4]. It is well known that the procedure requires the determination of the spacing, d_{hkl}, of a given crystallographic *hkl* plane in the stressed sample using Bragg´s law, $2d_{hkl}\sin\theta=\lambda$, where θ is the Bragg´s angle and λ the wavelength of the incident beam. Then, by using the formula,

$$\varepsilon = \frac{d_{hkl} - d_0}{d_0} \qquad (1)$$

the elastic strain, ε, in a given gauge volume is calculated in the same way as macroscopic strains are obtained in conventional mechanical testing with the help of a suitable extensometer. Direct use of the generalized Hooke´s law of elasticity, namely,

$$\sigma_i = \frac{E}{(1+\nu)(1-2\nu)}[(1-\nu)\varepsilon_i + \nu(\varepsilon_j + \varepsilon_k)] \qquad (2)$$

where σ_i is the *i* component of the stress tensor, related to the three strain components, ε_i, ε_j, and ε_k, E the elastic modulus, and ν the Poisson´s ratio, provides the stress state in the same way as a load cell measures applied loads in a testing machine. The attractiveness of using neutrons (or x-rays) is that a tri-axial stress state can be evaluated in a non destructive way. Then, the data obtained can be compared with the predictions derived from elaborated finite element codes or proposed models for subsequent assessment.

The crucial issue that makes the need for a very precise value of d_o so essential relies on the fact that small fluctuations or experimental errors in peak position can lead to huge variations of the calculated strain and resulting stress. For example, a variation of some few 10^{-14} m (or 10^{-3} Å) in the value of d_o (or *d*), say $2\text{x}10^{-14}$ m, can lead to a variation of the stress of the order of 10 MPa for the case of aluminum alloys. The stiffer the material the wider the variation (titanium, steel,…).

Usually, a guaranteed d_o value is obtained from powder of the same material, provided that powder does not hold a macroscopic stress. For this purpose, powder with a particle microstructure similar to that of the sample on which the RS is to be measured is required. In the case of many age hardening aluminum alloys, it is important, then, that both the powder and the sample had undergone the same temperature cycle to avoid the well known strong influence of the precipitation state on the lattice spacing of these alloys [5].

In many real cases, such as welds of these aluminum alloys, however, the above procedure becomes impractical since the temperature cycle undergone by the material is not known. It rather differs across the welded region; *i.e.*, "different" microstructures can be found across the weld. Such variations make it impossible in practice to apply the powder method to determine d_0. In cases like these, the so called "comb" sample method is used [3,6,7,8,9,10]. This method consists in sectioning the weld in small pieces or coupons so that the macroscopic RS, M-RS, is relieved. Then, the peak position obtained in each piece before and after sectioning can be compared and the M-RS profile calculated provided that the microstructure in the different pieces is not modified by the cutting operation. To ensure that the RS is relieved after sectioning, it is necessary that the dimensions of each piece are significantly smaller than the initial sample size or the *wavelength* of the M-RS to be determined. For practical purposes, the different pieces are not separated from

each other; they are, instead, kept together in the form of a comb in which each tooth keeps the specific orientation and d_0 value at that portion of the original weld with respect to a given coordinate system [6].

There are, however, several limitations to the comb method. First of all, one has to take into account the procedure itself. The measurements must be conducted first on the stressed sample. Then, the comb must be machined out to conduct further measurements for the d_0 determination: In this process, two set of measurements must be carried out necessarily in different experiments. This implies a different configuration of the instrument which can modify significantly the position of diffracted peaks. To avoid these inconveniences, it is common to extract a comb piece from the sample under study, so that both sample and comb can be studied in the frame of the same round of measurement using the same experimental set up [11]. This operation, however, inevitably leads to an alteration of the initial RS state to be studied.

Furthermore, several other considerations should be born in mind when using the comb method. Ganguly *et al*. [2] suggest that a retained macro-stress along the teeth direction of maximum dimension is still present in the comb sample, and to use it as a stress-free reference sample, the M-RS should be first determined. They propose, in agreement with [3], to measure near the tooth end using the $\sin^2\psi$ technique. They also found retained inter-granular strains along the transverse direction of the comb teeth. Huges *et al*. [3] scanned along the teeth of a comb specimen machined out from a 100 mm diameter quenched nickel superalloy cylinder. Measurements were conducted on several teeth; for the strain direction parallel to the long teeth dimension and for a perpendicular direction. They found no variation along almost the whole length of a tooth for the perpendicular strain direction, but found significant disparity along the teeth for the parallel direction. It was also found that there was convergence in data for the parallel direction at all teeth ends, and that value coincided with the value seen for the direction perpendicular to the teeth. They recommend conducting measurements as close as possible to the ends of the teeth, where data convergence was obtained.

In summary, the comb method may be of interest from a scientific point of view as it allows for further understanding of RS evolution/relaxation upon sample sectioning and/or machining. It is, however, undesirable from an engineering or practical approach; when the RS state of "real" components is sought. As a consequence of sample sectioning to obtain the comb, the attractiveness of the diffraction method disappears since it is, in fact, converted into a destructive technique. Nobody considers machining out a comb from a crucial component of an expensive device to study its RS state, particularly if it is planned to be in service again. Alternative procedures which account for reliable d_0 data to determine the RS state in real components such as welds of age hardening Al alloys, *e.g.*, 2xxx, are, therefore, desirable.

In the present study, the RS state resulting from a joint conducted by friction stir welding, FSW, in a AA2024 plate has been analyzed making use of equilibrium conditions (stress and bending moment) to obtain d_o. FSW is a very promising method for joining aluminum alloys in many industrial uses [12] and, like in other welding techniques, residual stresses are developed, affecting component performance. Two methods have been used to obtain d_o; first, equilibrium conditions have been imposed on sections parallel to the weld so that a d_0 value corresponding to the microstructure of the base material region can be calculated. Second, same conditions were imposed on a cross section transverse to the weld. Here, an analytical solution is impractical because d_0 values vary across the weld, *i.e.*, a large number of variables is involved. The different d_0 values across the weld were obtained using a genetic algorithm, GA, which is a simplified case of evolutionary algorithms, EAs. Such a method is able to handle problems in which many variables and possible solutions are involved. EAs operate in the field of evolutionary computation, which emerged in the late 1960s when the possibility of incorporating the natural mechanisms of selection and survival, in accordance with Darwinian evolution, to solve Artificial Intelligence problems was proposed [13]. An important factor of natural selection is the appearance of small variations, which are both random and directionless in phenotypes. These variations, usually referred to as

mutations, can survive the selection if they prove their value in the environment of the species. These search and optimization algorithms have lately extended their capacity to solve very different problems in materials science [14]. For example, a GA together with a finite element code, has been used to simulate the FSW process of aluminum alloys 6005A-T6 and 2024-T3 [15].

~~Furthermore, conventional measurements in a comb sample machined from a second plate were carried out.~~

2.- Materials and experimental procedure

The aluminum alloy used in this investigation was AA2024 in the form of a 10 mm in thick plate, supplied by Alustock in a T351 condition [T3, Solution Heat Treated, Cold Worked, and Naturally Aged to a Substantially Stable Condition. T3 applies to products that are cold worked specifically to improve strength after solution heat treatment and for which mechanical properties have been stabilized by room-temperature aging. It also applies to products in which the effects of cold work, imparted by flattening or straightening, are accounted for in specified property limits. T*x*51 applies specifically to plate, to rolled or cold-finished rod and bar, to die or ring forgings, and to rolled rings. These products receive no further straightening after stretching [20] pg. 115-116]. For this investigation, two pieces of 296x150 mm^2 were cut in order to perform ~~two~~ a butt welds~~,~~ of about 250 mm in length, ~~under the same welding conditions~~. ~~In this way it was ensured, in principle, that the microstructure developed in the different regions of the two welds was similar.~~
The weld was made with no additional mechanical/chemical preparation of the surface edges which were joined: simply the usual finishing from the mill was made to eliminate defects from the cuts. The welding experiment~~s~~ was conducted at AIMEN, Porriño, Spain, making use of a PDS-4 Intelligent Stir FSW machine from MTS. The welding conditions were: 400 rpm of rotational speed and 100 mm/min of advancing speed. The tilt angle was 1.5°. A 2-piece fix tool with a threaded pin (7.62 mm long) which included three ground flats was used. The shoulder diameter was slightly above 20 mm while the pin diameter varied from 7.95 to 6.35 mm. The internal face of the shoulder was not flat, but inclined by 7° to create a conical surface. The shoulder and the pin were made of H13 steel (48 HRc) and MP159 alloy, respectively.

~~The first welded plate was used to~~ To investigate the RS state across the weld ~~For this purpose~~, d_{311} (where sub-index denotes crystallographic plane) ~~across the joint~~ was extracted from neutron diffraction experiments at three different depths: -2.5, -5, and -7.5 mm from the surface on which the tool pin entered the plate (top surface), denoted hereafter as front, center, and bottom regions. The region measured covered up to ±85 mm on both sides from the center of the weld, in the transverse direction of the plate. In this way, a complete scan across the weld, including the nugget, the thermo-mechanically affected zone, TMAZ, the heat affected zone, HAZ, and the base material, BM, on both sides of the weld was performed. Since the plate was not sectioned, it is guaranteed that no modification of the M-RS has occurred.

~~On this plate,~~ Also measurements of d_{311} across two different longitudinal sections, located at 52 mm and 120 mm from the center of the weld, on the retreating side, on five locations along the plate and at six depths, namely; -1.2, -2.7, -4.2, -5.7, -7.2, and -8.7 mm, were ~~also~~ conducted. Figure 1a) is a scheme of the welded plate showing the location across the weld where the M-RS state was studied and the two longitudinal sections on which d_{311} measurements along the three principal directions were carried out. As seen in the figure, both sections correspond to the base material where microstructural variations are insignificant. Measurements were made on two different sections to ensure the reproducibility of the results. A Cartesian reference system was adopted, where the origin is located in the center of the welded plate, on the top surface, and the axes coincide with the longitudinal (rolling), *L*, transverse, *T*, and normal, *N*, directions of the plate (Fig. 1a). Due to the limited beam time allocated for this kind of experiments and the typically long time required to obtain reasonable peak signals by neutron diffraction, only measurements for the principal directions were possible. Finally, $\sin^2\Psi$ scans (with Ψ the angle between the scattering vector and the normal plate, *N*, direction) were conducted at different locations of the weld to ensure whether or not the sample reference system is a principal directions one.

~~The second welded plate was used to machine out a comb reference sample and to study the microstructure and texture of the plate. The location from which the comb was extracted (by electro-discharge machining) was nearly the same as that on which d_{311} measurement across the weld in the first plate were made. So, it was also expected that, despite the changes due to the temperature/strain cycle gradients associated with the FSW process, the microstructure at the different locations across the first weld and the corresponding ones in the comb sample would be the same. Figure 1b) shows the comb sample used in this research. The free ends of the teeth coincide with the top surface.~~ Conventional metallographical procedures were used to examine the microstructure by optical microscopy. The texture was determined by the Schulz reflection method using laboratory x-rays, as described elsewhere [16].

The d_{311} measurements were performed on SALSA diffractometer of the ILL (Institute Laue Langevin), in Grenoble, France. This instrument is most suitable for measuring RS in real components used in engineering provided a hexapod that can hold, move, and rotate large and heavy samples, up to some 1000 kg, with high precision (5 μm) [17]. Figure 2~~a)~~ shows a general overview of the instrument with the AA2024 welded plate mounted on the holder, ~~and Fig. 2b) is a detail of the plate studied~~. Further details of this diffractometer are in [17,18]. The wave length of the neutron beam was λ=1.699 Å, selected by a double focusing silicon bent crystal monochromator. The Al(311) has been used because it represents well the bulk behavior of the material and is less effected by crystallographic texture [19]. The resulting Bragg angle for the diffracted peak used was around 2θ=88°. The scattering plane, that defined by the incident and diffracted beams, lies in the horizontal plane of the instrument. The elastic modulus used for the RS calculations was taken as the average between the tension, 72.4 GPa, and compression, 73.8 GPa, values, and the Poisson ratio was 0.33 [20].

Due to the limited rotations of the hexapod and the sample shape, the measurements were made in two steps. The plate, placed in a vertical position, was measured under two configurations. First, with the weld in the vertical direction so that a 90° rotation about a vertical axes (perpendicular to the scattering plane) allowed for the measurement at *N* and *T* directions. Second, with the weld located horizontally, in which case, the 90° rotation about the same vertical axes makes it possible to determine d_{311} for *L* and *N* directions. Two different gauge volumes were used to optimize the beam time allocated for this experiment. For the first case (weld in vertical position) a gauge volume of 2x2x24 mm^3, where the longest direction coincided with the vertical one (rolling direction), was used. It was possible to use this large gauge volume because the microstructural variation along the weld and corresponding RS state is minimal. For the second case, a smaller gauge volume, 2x2x2 mm^3, was used to avoid possible microstructural gradients and RS variations inside the gauge volume. The gauge volumes were defined by radial focusing collimators made of Gd coated Mylar foils.

~~For the case of the comb sample the same two configurations (weld in vertical and horizontal directions on the holder) were employed to measure the lattice spacing for the three principal directions. In this case, however, all measurements were made with the same gauge volume of 2x2x2 mm^3.~~

3.- Experimental results

3.1.- Microstructure

Toda esta sección hay que rehacerla!

The resulting microstructure of the weld is shown from the transverse metallographic section in Fig. 3. In this figure, the microstructures of the different regions developed during FSW are clearly discernible: In the nugget or recrystallized region, an even distribution of small equiaxed grains, of about 4 μm, is appreciated. The boundary between the nugget and the thermo-mechanically affected zone, TMAZ, is very sharp on the advancing side, but becomes more diffuse in the retreating one, which reveals the non-symmetrical nature of

the FSW process. The microstructure developed on the TMAZs results from the combined effect of temperature and deformation. This leads to elongated grains in the direction of the material flow and an over-aged, coarse, precipitation. The microstructure of the heat affected zone, HAZ, is characterized by the same grain structure as that of the base material, with an average grain size of 17 μm and an aspect ratio of 4:1. This microstructure results from the cold rolling process undergone by the original plates. Additionally, the temperature rise in these zones makes the fine semi-coherent precipitates of the T6 state evolve into coarse less reinforcing phases such as the η ($MgZn_2$) one [21,22].

The texture of the as-received AA7075 plate is described as inverse stereographic triangles (*N* direction) corresponding to the center and outer regions of the plate, Fig. 3b). As can be seen, a texture gradient, typically appearing in rolled aluminum alloys [23], is developed. The [011] component which appears in the center region is absent in the near-surface regions of the plate. The texture developed in the plate is not too intense: The maximum corresponds to the [100] component in the outer region, where an intensity of about 3 times the random one is obtained. In spite of the not too intense texture, the presence of a gradient suggests not only a variation of the inter-granular RS through the plate thickness but also that the usual approximation of plane stress conditions for RS calculation is not recommended.

3.2.- Neutron diffraction measurements

The results of the d_{311} values obtained across the welded plate, for the three components, *L*, *N*, and *T*, and at the three depths, front, center, and back, are summarized in the plots of Fig. 4. For any component, the shape of the profile does not vary substantially with plate depth. Also, the profiles of the *L* component are M shaped in agreement with other investigations [7,24,25,26], with a total variation of $\Delta d_{311} \approx 0.0025$Å, which corresponds to some 2450 μ-strains. The d_{311} value remains nearly constant in regions away from the weld, but increases rapidly as the weld is approached up to a maximum and then decreases down to a minimum located at the center (nugget) of the weld (*X*=0). The *N* and *T* components, however, are W shaped, and the total variation in d_{311} is slightly smaller than for the *L* component: the total variation corresponds to about 1800 and 1500 μ-strains for the *N* and *T* components, respectively. These profiles are, again, commonly observed in FSW of aluminum alloys [25]. The significant d_{311} variation across the weld for the *N* component should not only be attributed to microstructural changes due to the FSW process [5], but also to the presence of a RS. This confirms that a biaxial stress approach is not valid here, as suggested above. ~~For comparison, the corresponding values obtained from the comb are also included in these plots. The total range of variation of the lattice spacing in the comb is of $\Delta d_{311} \approx 0.0017$ Å, corresponding to about 140 μ-strains. It can be seen from the figure that the d_{311} values in the nugget of the plate and the comb for the *L* component are very similar. However, in regions distant from the nugget and for the whole *N* and *T* profiles the d_{311} values on the comb are significantly higher than on the plate.~~

The results of the d_{311} values in the longitudinal sections at *X*=52 mm and for the three directions (*L*, *N*, and *T*) and at different plate depths are summarized in the plot of Fig. 5. The close values obtained for the different depths suggest that the through-thickness gradient is not relevant. It is also seen that the d_{311} variation along *L* is very smooth. No significant differences between the profiles obtained at *X*=52 mm and *X*=120 mm (not shown in this figure) was appreciated. ~~The d_{311} value obtained from the comb at *X*=52 mm is also represented in these plots as dotted lines for direct comparison. It can be seen that the comb data are always above the data along the sections.~~

The $\sin^2\Psi$ scans led to reasonable linear 2θ dependences, which confirm that the coordinate reference system selected, that of the rolled plate, is a system of principal axes. For the sake of simplicity, plots of these data are not presented.

4.- The genetic algorithm

A GA works with a population of individuals, where each individual represents a potential solution to a problem. The basic idea is to evolve an initial population (or representations of solutions) randomly generated, forcing it into a repeated process of selection, crossover, and mutation. Each cycle or process gives rise to a generation. The objective is to find the individual that, over a certain number of generations, best approaches the optimal solution. As follows, a Multi-objective Genetic Algorithm has been implemented to obtain d_0 profiles across the weld which minimizes both the sum of longitudinal stresses and bending moments in the transverse section, according to a protocol described in this section.

Using the smallest distance between neutron diffraction measurement points, the whole transverse section of the welded plate was divided into 181 zones. The actual measurements made in the regions away from the weld were more spread out than in regions close to the nugget, and the very extreme regions were not scanned since the time available for the experiment at SALSA had to be optimized. Since these regions were not affected by the FSW process, it was assumed that their d_{311} values were similar (the average of the measurements made in the base material). In principle, the procedure was as follows: Each zone was specified by nine parameters corresponding to the three depths (front, center, and bottom) and the three components of the stress (*L*, *N*, and *T*). Therefore, a chromosome (string of numbers representing the solution) composed of 181 x 9 =1629 genes (positions) was used. The first nine genes represent the parameters for the first zone, *i.e.*, $d_{0LFront}$, $d_{0TFront}$, $d_{0NFront}$, $d_{0LCenter}$, $d_{0TCenter}$, $d_{0NCenter}$, d_{0LBack}, d_{0TBack}, and d_{0NBack}), the next nine the parameters for the second one and so on. According to the results obtained from the comb, however, it was assumed that no anisotropic effect on the d_0 value exists: *i.e.*, the same d_0 value is obtained, irrespectively of the sample direction. Therefore, the final chromosome was composed of 543 genes. A randomly generated set of solutions, or a set of strings of numbers, was used as the starting point. Finally, a population size of 8000 individuals, 2000 generations, 0.1 % mutation probability, and 80 % crossover probability was used in the present analysis.

5.- Discussion

~~As it can be seen from Figs. 4 and 5, there are important differences between the set of d_{311} values in the plate (across the weld, Fig. 4, and in the longitudinal sections, Fig. 5) and the comb. In other words, the d_{311} data in the comb are significantly larger than in the plate. These large differences lead, readily, to the result that a compressive stress would be obtained virtually in the whole plate. Such a surprising result is in contradiction with the elementary principles of Mechanics. There are several possible reasons to account for this:~~

~~1.- The fact that the comb was machined from a different plate from the one where the RS was investigated: it may be possible that the precipitation and solid solution state differs from one weld to the other despite the fact that similar parameters were used in both welds. It appears that even in apparently well controlled FSW operations, it is difficult to reproduce the precipitation and solid solution state in these welds, a factor strongly influencing lattice spacing values. The circumstance is similar to that shown in some previous research [27], where the complexity in analyzing creep data in age hardening aluminum alloys has been pointed out. Due to the un-controlled precipitation process which occurs during testing, it is difficult to make a rigorous analysis of creep data obtained at different temperatures and in different laboratories of a given age hardening alloy [27].~~

~~2.- It could also be possible that full RS relaxation has not occurred in the comb, or that comb preparation has induced extra residual stresses [2,3].~~

3.- Finally, different stress relaxation from one plate to the other could be the reason for the above result [28]. In conclusion, although both the comb and the welded plate can lead to reliable results, the former cannot be used as an un-stressed reference for the latter: they should be treated as separate problems.

5.1. Comb sample

Although the comb is revealed as a non reliable un-stressed reference in this experiment, the results supplied can still be of great help for a rigorous analysis of the RS state in the weld. For a better comparison of the data, the values for the three components are shown together in the plot of Fig. 6. As can be seen, the d_{311} values for the *L*, *N*, and *T* components only coincide in the nugget and TMAZ regions, whereas they split apart in the HAZ and the BM (the error was ≈45 μ-strains). Although the difference is small, the lowest d_{311} value corresponds systematically to the *L* component and the highest to the *T* one. This trend is similar to that obtained by Ganguly *et al* [29] in 2024Al alloy plate. The differences lead to about 125 μ-strains, a value significantly smaller than the variations obtained by Steuwer *et al* [5] (of about 2000 μ strains considering the maximum variation of their un-strained lattice spacing) or by Linton and Ripley [28] (of about 3750 μ strains from the 2θ variation data across the weld) in combs machined from welds of 7xxx alloys. It is surprising that, despite these large differences, no conclusive justification is given to explain these results. In the present case, and in agreement with [29], the difference is attributed to a (microscopic) inter-granular stress originated during the rolling process of the initial plate (inter-granular stresses do not relax upon sample sectioning if the comb teeth are significantly larger than the grain size). As a consequence of the plain strain condition imposed during rolling, grain elongation and crystal grain rotation occurs in a non uniform manner. As a result, a texture (and texture gradient through the plate thickness, Fig. 3) is developed where grains have deformed differently, depending on their final crystal orientation: *i.e.*, although the total strain, that imposed by the rolling process to obtain the final plate [30], is the same in all grains, the strain partition between plastic and elastic components differs from grain to grain, and depends upon lattice grain orientation. This elastic strain difference is the origin of an inter-granular stress. Subsequent heat treatments, such as the one to reach a T6 condition, do not relieve this stress. Only in the nugget region (where full recrystallization has occurred) and the TMAZ the d_{311} values for the three principal directions coincide. This is consistent with the fact that new grains are being formed, a random texture is obtained, and the inter-granular stress developed in this region during rolling disappears. The presence of an inter-granular stress adds further complexity to the determination of the M-RS resulting from the welding operation on the basis of measurements conducted in comb samples.

5.2.- Equilibrium conditions

Procedures based on equilibrium conditions of macro-stresses [31] have, then, been used to calculate appropriate d_0 values for residual stress determination. On the basis that the AA2024 alloy can be considered a single-phase material, like all 2xxx alloys, the contribution of second phase particles and the required stress equilibrium with them are neglected in the analysis. Therefore, it is assumed that the measurements conducted correspond to actual macroscopic stresses, as made in other works [4,5,6,28].

The use of equilibrium conditions is a very rigorous procedure, which furthermore avoids the tedious operations and approximations involved in the comb method. It is surprising, however, that it has not been sufficiently exploited in the past [32,33]. The condition of equilibrium implies that, on any section of the component, *S*, the total force perpendicular to it and the bending moment of the in-section forces with

respect to the neutral plane, *N*, should be zero. For the present case, a plate in which one of the dimensions, *Z*, is significantly smaller than the other two dimensions, *X* and *Y*, Fig. 1, bending is possible only about an in-plane axes. Then, the equations describing this equilibrium in a general form are integrals [31], which can be substituted by summations since only discrete measurements were taken in the experiment. Therefore, the equilibrium is given by,

$$\sum \sigma_{\perp} \Delta S\Big|_S = 0 \tag{3}$$

and for the bending moment, *M*,

$$\sum M\Big|_S = \sum \sigma_T \, \Delta S \, Z_n\Big|_S = 0 \tag{4}$$

Where Z_n refers to the distance from the neutral plane of the plate.

Of course, also local equilibrium within the plate should be satisfied. To apply this condition, however, a description of the stress variation along the three spatial directions would be needed. Since measurements on specific sections of the plate were conducted, only stress variations on two directions are possible. Therefore the above condition cannot be applied.

Two different approaches, as above mentioned, are here presented. First, taking advantage of the measurements conducted on the longitudinal sections (retreating side), at *X*=52 mm and *X*=120 mm, Fig. 5, balance conditions are imposed to seek for a constant d_0 corresponding to the BM. Second, equilibrium is applied to the transverse section, across the weld, where a variation of the un-stressed lattice parameter is expected due to the ageing nature of the AA2024 alloy.

5.2.1-Equlibrium on longitudinal sections of the plate

In this case, equilibrium, in accordance with equation (3), should be found for σ_T. Then, using equations (1) and (2), it must be,

$$\sum \frac{E}{(1+\nu)(1-2\nu)}[(1-\nu)\frac{d_T-d_0}{d_0}+\nu(\frac{d_N-d_0}{d_0}+\frac{d_L-d_0}{d_0})]\Delta S\Big|_{X=52,120} = 0 \tag{5}$$

Since a unique d_0 value is sought, an analytical solution of equation (5) is possible. Solving for the two sections, it is obtained; d_0= 1.22228 Å, at *X*=52 mm and d_0= 1.22232Å at *X*=120 mm. The small difference between these values accounts for their validity. Their soundness is further supported by imposing the equilibrium of the bending moment, as dictated by equation (4). For this case, equation (4), as applied to the longitudinal sections, turns into,

$$\sum \frac{E}{(1+\nu)(1-2\nu)}[(1-\nu)\frac{d_L-d_0}{d_0}+\nu(\frac{d_N-d_0}{d_0}+\frac{d_T-d_0}{d_0})]\ \Delta S\ Z_n\Big|_{X=52,120} = 0 \tag{6}$$

Using the average d_0 value resulting from those obtained at *X*=52 mm and *X*=120 mm of 1.22230 Å, it is found that the total bending moment, *M*, for these two sections is -110.8 Nm at *X*=52 mm and -22.3 Nm at *X*=120 mm. The values are not null, but are reasonably low considering that a discrete summation of data, obtained from the experimental results, rather than a rigorous integral of a continuous description of the stress has been made. It should be borne in mind that it is not analytically possible to find a unique solution which satisfies, both, equations (5) and (6) simultaneously. It is also worth mentioning that this un-stressed lattice

parameter is not influenced by the presence of the inter-granular stress (microscopic) ~~revealed in the previous section by the comb.~~ This micro-stress, of "wave length" much smaller than that of the macroscopic stress, overlaps the latter one, but does not modify its profile through the sample, and must be self-equilibrating.

The average d_0, together with the d_{311} data of Fig. 4 and equations (1) and (2), were used as a first approximation to obtain the RS profiles across the weld. The results obtained are shown in the plots of Fig. 7 where the RS profiles for the *L*, *N*, and *T* components at the three depths are presented. As can be seen, profiles similar to those obtained in other research works are obtained [6,18,28]: the stress in the *L* direction shows the largest absolute value (positive) and is similar for the three depths.

With this value, it is possible to determine if the *L* component of the stress for the section perpendicular to the weld also satisfies the balance condition. The total stress calculated is above 10300 MPa, and the bending moment is 103.8 Nm, values which are away from equilibrium. This result is not surprising since the expected variation of d_0 across the weld, nugget, TMAZ, and HAZ regions, is not taken into account in this calculation.

5.2.2.- Equilibrium on a transverse section of the plate using a genetic algorithm

Despite that the above method leads to a reasonable RS profile, Fig. 7, equilibrium across the weld is not reached. It is, therefore, necessary to take into account that d_0 is not constant through the weld for a rigorous description of the RS state. The BM has a uniform microstructure and therefore, the d_0 calculated in section 5.2.1 for this region can be considered as a valid one. On the contrary, the nugget, the TMAZ and the HAZ undergo microstructural changes produced by the welding process that affect considerably the unstrained lattice spacing. The use of the stress balance condition on a section with a variable d_0, implies a great number of unknown quantities, which cannot be calculated by an analytical method such as the one used in previous section.

For this case, the implementation of EAs can be of great help due to their capacity to handle problems in which a large number of unknown quantities are to be determined. In the present study, we pursue a string of d_0 values which vary in the welded region as a consequence of the severe thermo-mechanical process introduced by the FSW. Here, it is important to notice the restrictions imposed on the possible d_0 values in the different weld regions: They should lie between the maximum and minimum *d* values given by the plots of Fig. 4. This restriction is correct under two assumptions: a) the possible hydrostatic stress component is negligible, and b) the inter-granular stress is also insignificant. The first one is in principle supported by the known fact that welds do not lead to a significant hydrostatic stress, as revealed by the RS profiles obtained in previous investigations [11,28,34]. ~~The second one is supported by the results obtained from the comb measurements, Fig. 5, and the analysis of section 5.1.~~

To obtain the best set of d_0 values for each one of the 181 zones after the iterative procedure of the GA, equation 3 and 4 should be obeyed using the different chromosomes and the experimental data of Fig. 4 (the searching process was simplified by using only eight intervals in the welded region and the constant d_0 value calculated in section 5.2.1 for the BM). The iterative procedure was repeated 30 times to ensure the reproducibility of the final result. The GA has been implemented and run in Java, using an Intel core i-5, 4GB RAM memory running under Windows 7. The average total execution time for a population of 1000 Individuals and 500 generations over 30 runs was of about 100 seconds and the average evaluation time of one individual was nearly two tenths of a millisecond. A progressive decay of the total stress as a function of the number of iterations was obtained, which supports the validity and uniqueness of the result. It is worth mentioning that once full convergence was reached no further change in the final result (string of d_0 values) was required by the GA. The average of the 30 solutions resulting from the GA is summarized in Fig. 8, where the d_0 profile across the weld is shown. The highest values are obtained in the base material, whereas in the HAZ, TMAZ, and

nugget a clear drop results. In summary, a W type of profile in the welded region is obtained, where the minimum is reached near the TMAZ zones and the maximum in the nugget region.

The d_0 values provided by the GA, Fig. 8, are consistent with the precipitation state in the BM, HAZ, TMAZ, and nugget. Considering that the plates underwent a peak-aged treatment, the lattice spacing must be increased by the coherent precipitates (mainly η') [21,22]. The temperature rise in the HAZ and TMAZ zones modifies the initial precipitation state to an over-aged one (mainly incoherent coarse η precipitates). In these conditions, the lattice spacing is "relaxed" to its lowest value. Finally, the FSW induced recrystallization process modifies the microstructure of the BM leading to a grain boundary η precipitates and a fine dispersion of Guinier-Preston, GP, zones and η' precipitates inside grains [21,22]. This microstructure results in intermediate lattice spacing. Therefore the d_0 profile across the weld is expected to have a W shape, which somewhat agrees with the result of Fig. 8. It is also seen that the d_0 profiles across the plate (front, center, and back) differ from each other, which is an indication that the friction occurring only on the top surface induces a through-thickness gradient of the thermo-mechanical process

The final RS profiles calculated using the d_0 values given in Fig. 8 are shown in Fig. 9. The profiles resemble a M shape for the longitudinal component and a W shape for the transversal and normal components, as reported in former works [4,25,35,36,37]. The highest tensional RS was found in the longitudinal component, in agreement with previous studies [25,26,37] and reached about 74% of the yield strength of the BM, which ~~lies within the ranges~~ exceeds the 20-70% range reported in [~~10~~ 25]. The asymmetry of the FSW process is also reflected in the RS profile, the maximum was located in the TMAZ of the advancing side. Depending on the material and the welding parameters, the location of the maximum RS was reported in the HAZ [4,25,26] or the TMAZ [10,36,37]. The profiles corresponding to the back region, Fig. 9, showed the highest RS levels, which decay progressively, first in the center and, then, in the front regions. In the latter one the profile shows the smoothest RS profile. This trend is more evident in the *T* and *N* components and is consistent with the idea that the macroscopic RS generated by FSW is maximum in the back region, where the temperature reached is not as high as in the front region, where partial RS relaxation may have occurred.

When comparing the RS profiles of Figs. 7 and 9 it can be seen that the maximum stress is higher in the second case. In other words, the RS obtained using a constant d_0 value underestimates the actual RS state in the plate, as obtained from the GA. Not taking into account this difference in engineering design could lead to dramatic consequences during weld service.

6.- Summary

In this research an analysis of the d_0 value needed to calculate the macroscopic residual stress across a weld conducted by FSW in AA2024 plates has been made. ~~In parallel, measurements of the inter-planar distance in a comb sample machined from a second plate welded under identical conditions were also made. The disadvantage of the comb method lies in the fact that the sample/component on which the residual stress is of interest must be sectioned. It has been shown that if the comb is machined from a "twin" weld, minimal and uncontrolled variations of the precipitation state are enough to distort the real un-stressed reference. Furthermore, the presence of inter-granular stresses, not relieved in the comb, further complicates the determination of a reliable d_0 value.~~ As an alternative to the comb method, two procedures based on equilibrium principles have been used to recalculate a suitable un-stressed reference. The first one makes use of a constant d_0 value calculated from the equilibrium conditions applied to longitudinal sections, parallel to the weld. Here, an analytical solution can be derived given that a unique d_0 value, that corresponding to the base material, is the unknown variable. The un-stressed lattice parameter obtained is not affected by the inter-granular stress since it must self-equilibrate: It overlaps the profile of the macroscopic residual stress. Since a constant d_0 is used, the RS obtained across the weld (*L* component) and the bending moment is not

equilibrated, despite that the profile is reasonably similar to those obtained in previous research works. The second one uses a genetic algorithm to find the equilibrium across the weld (transverse section). In this case, the applicability of the analytical method, as done in the longitudinal section, is not possible given that d_0 varies through the weld due to the presence of different microstructural regions which underwent different themo-mechanical cycles. The only requisites imposed on the GA is to minimize the summation of stresses perpendicular to the section under study and the bending moment about an axis parallel to the weld. With this method, d_0 values for the different regions, namely, the nugget, the TMAZ and the HAZ, are selected from values which range in the interval given by the maximum and minimum values measured in each region. With the resulting d_0 profile, a final RS state across the weld is obtained, where the d_0 oscillations due to the microstructural variations in the weld are taken into account. The RS obtained (*L* component) with the constant d_0 value underestimates the calculated RS resulting from the GA.

Acknowledgements

Support from Projects MAT-05-0527 and MAT-09-09545 from MICINN, and PIE 200960I076 from C.S.I.C., Spain, is gratefully acknowledged. Financial help from the ILL to conduct the neutron diffraction measurements on SALSA, experiments 1-02-6 and 1-02-10, is recognized. Support from Spanish Government grants TIN 2008-00508 and MEC CONSOLIDER CSD00C-07-20811 and from Spanish MINECO (projects MAT2011-23455 and MAT2011-25991) is also acknowledged by J.I.H. and I.P.O., respectively.

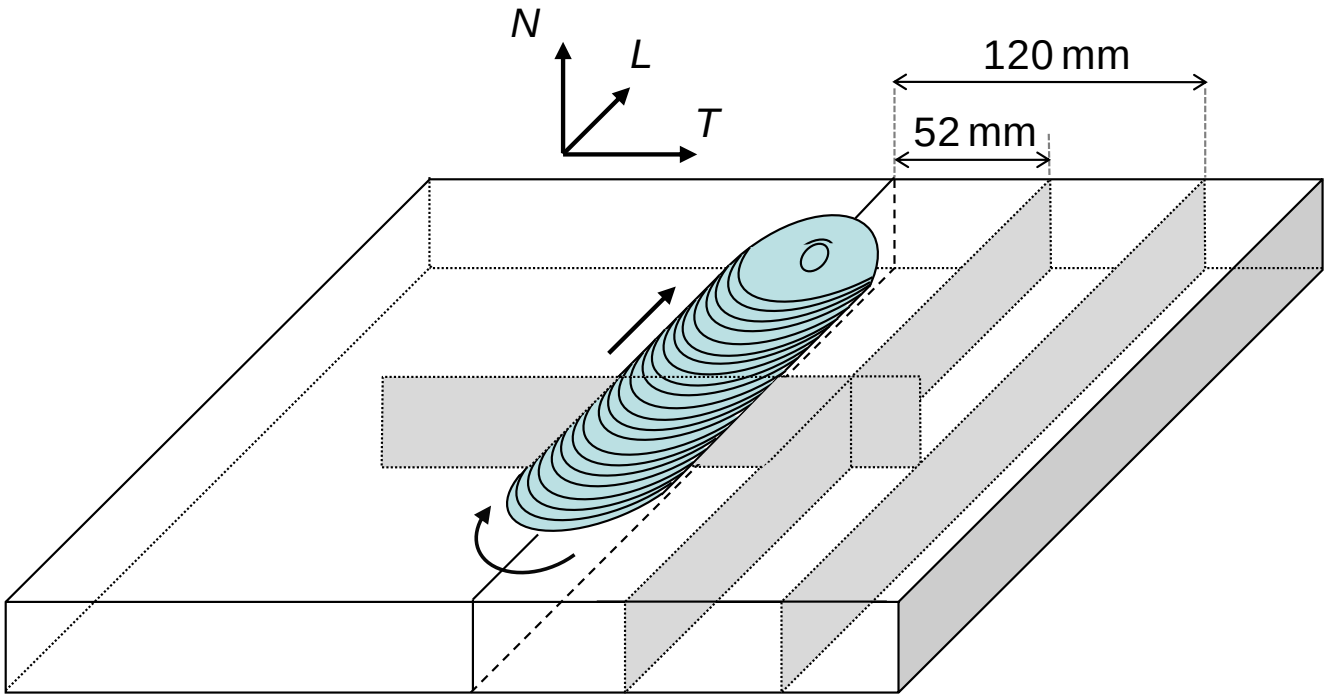

Figure 1.- Scheme of the welded plate showing the location on which the RS state was studied and the two longitudinal sections on which d_{311} measurements where conducted. Directions *T*, *L*, and *N* of the reference system coincide with axes *X*, *Y*, and *Z*, respectively. ~~b) Comb sample machined across the weld of the second plate (close to the same region where the RS state was studied in the first plate).~~

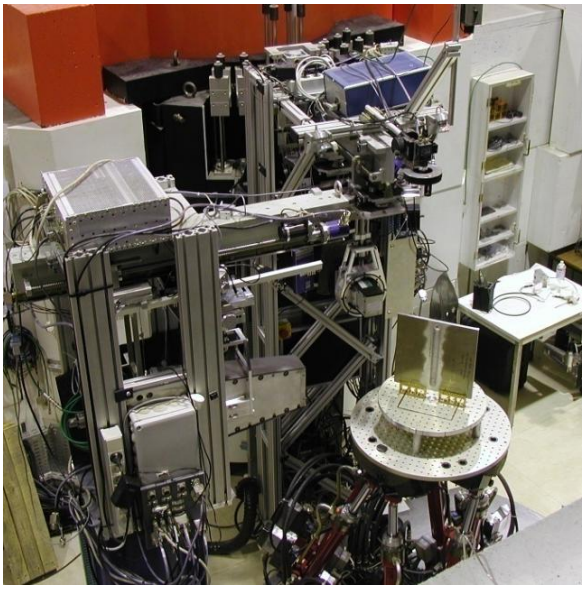

Figure 2.- a) Experimental set-up of SALSA instruments showing the AA2024 welded plate mounted on the hexapod. The welding line is parallel to the rolling direction. QUITE LA B

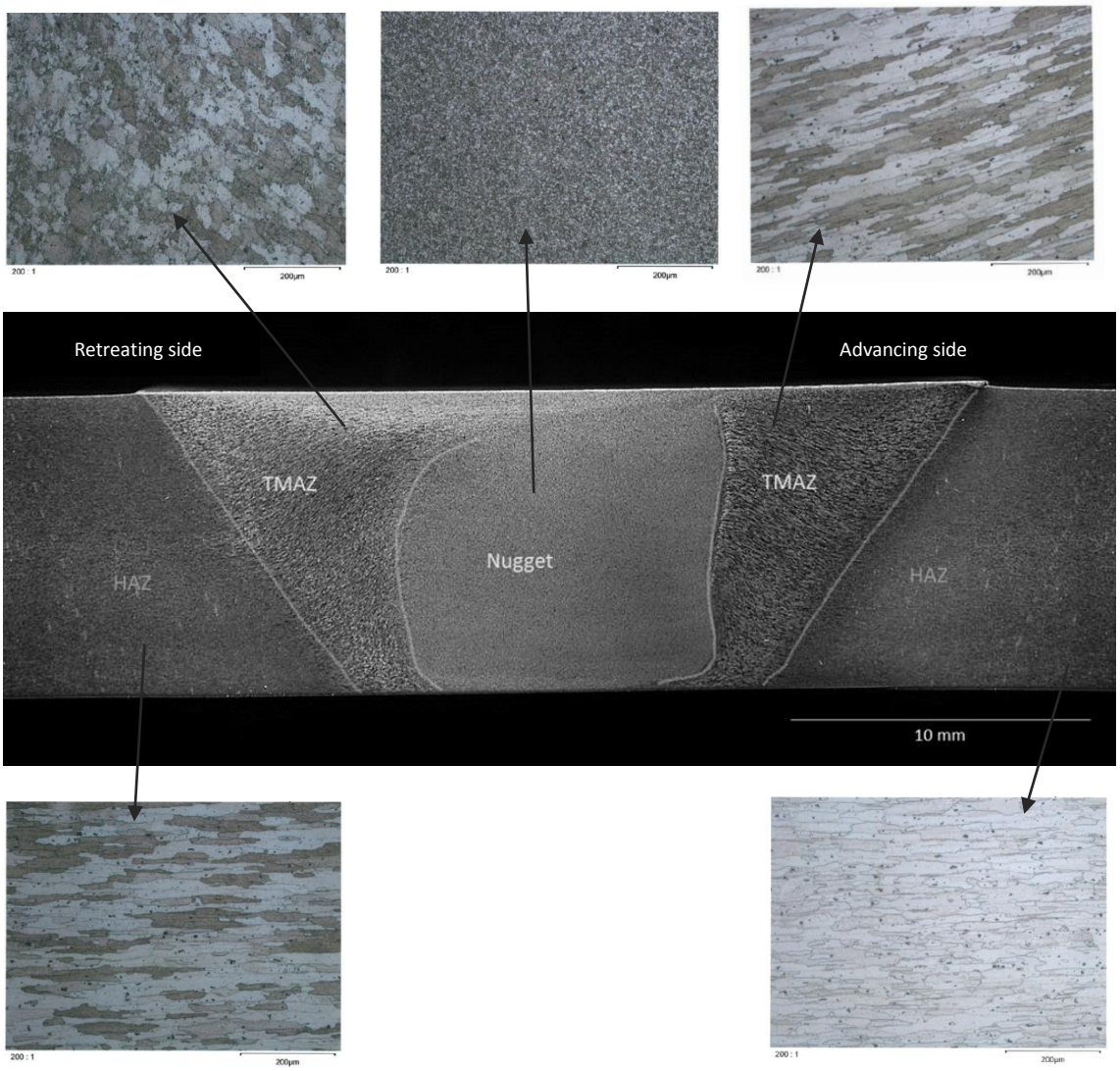

a)

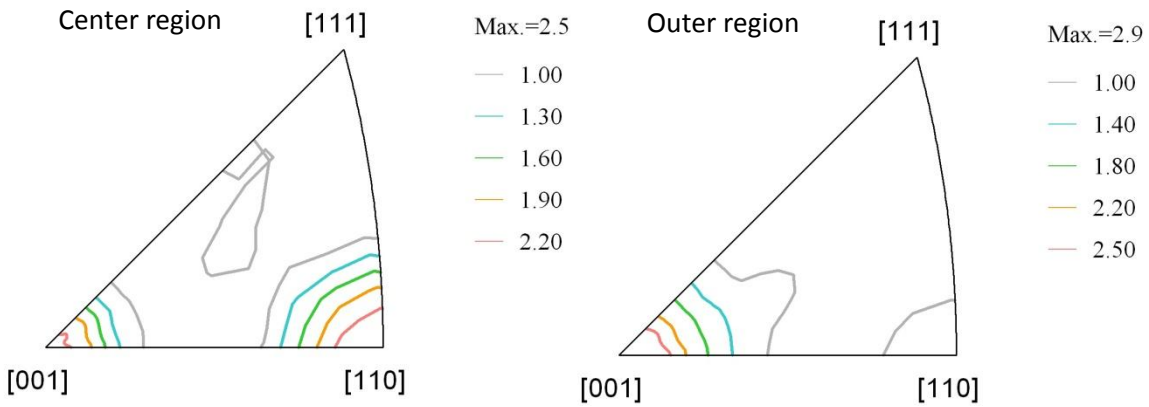

b)

Figure 3.- a) Transverse metallograpical section of the weld showing the microstructure developed in the different regions. b) Texture of the as-received AA2024 plate represented as inverse pole figures for the *N* direction at the center and outer regions. REHACER Y REEMPLAZAR

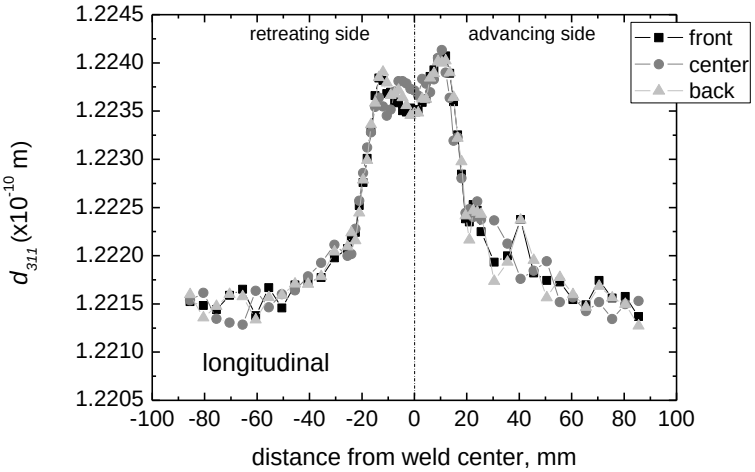

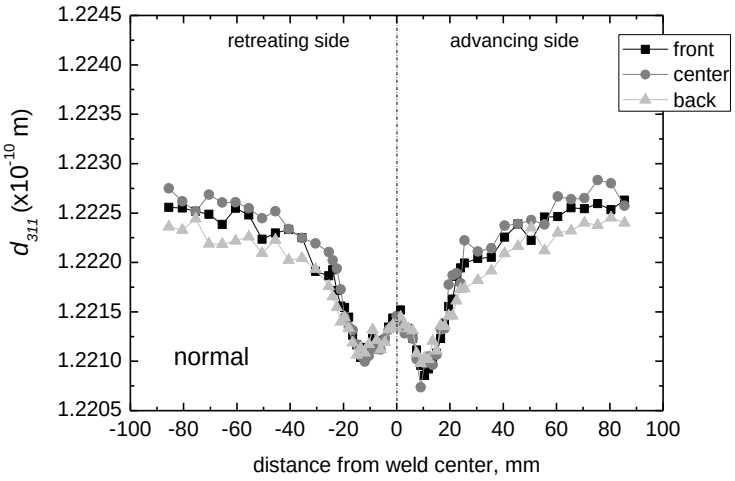

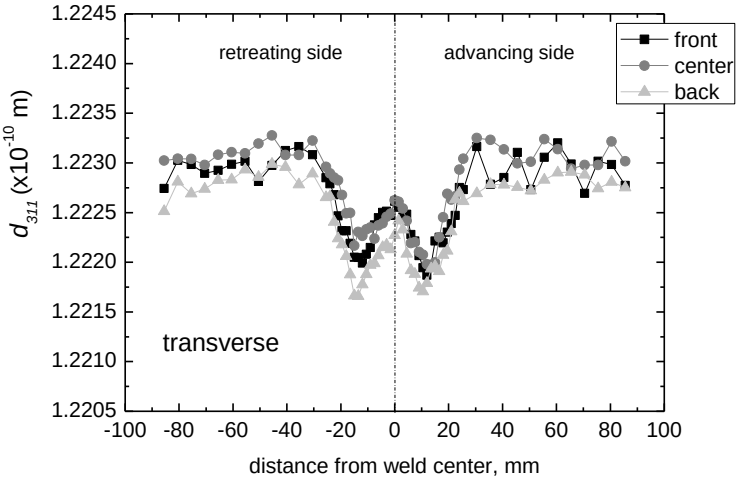

Figure 4.- Inter-planar distance data, d_{311}, as a function of distance from the center of the weld, at the three different depths; front, center, and back, for the three directions *L*, *N*, and *T*. ~~For comparison, the data obtained from the comb sample is also included (error is of about ±0.0007 Å).~~ QUITÉ COMB!

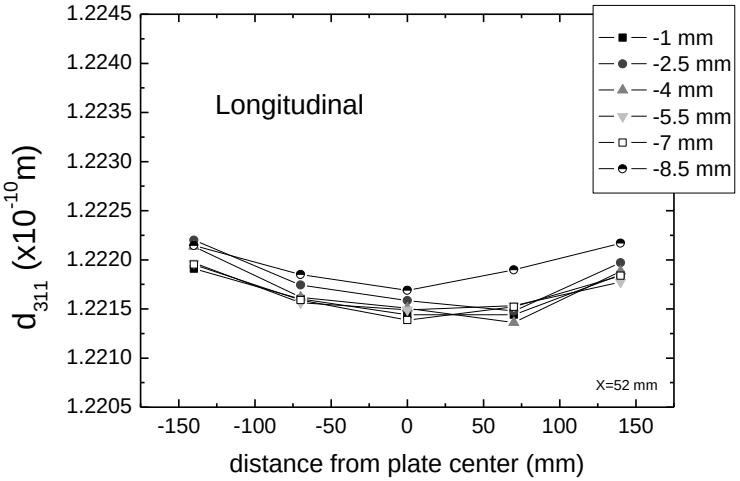

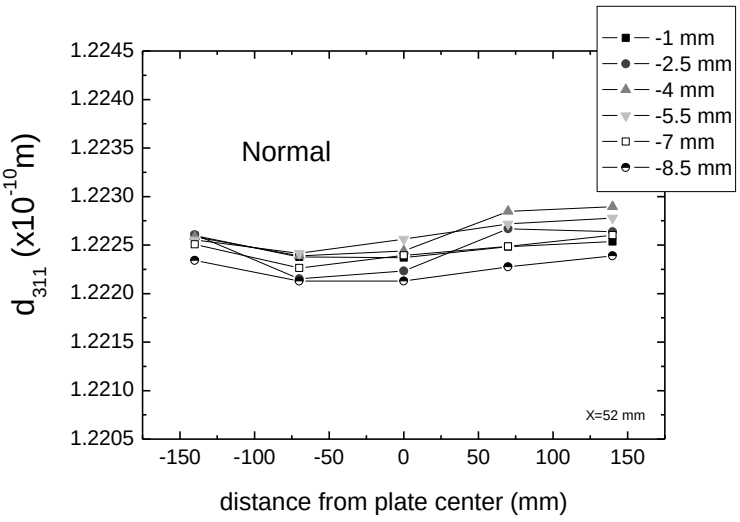

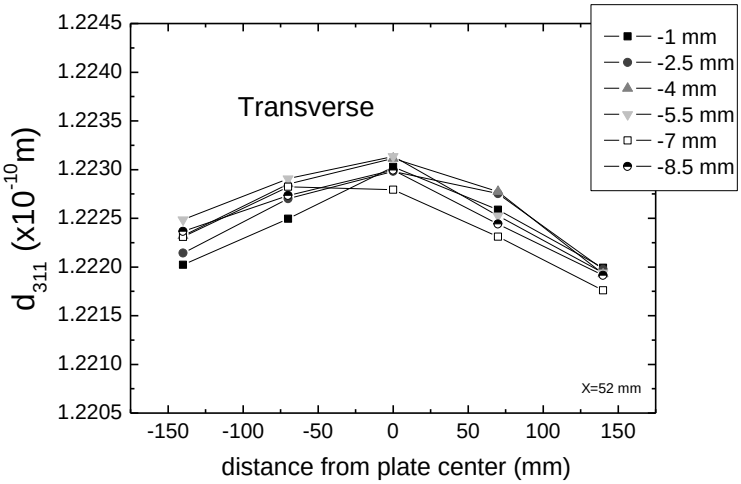

Figure 5.- Inter-planar distance data, d_{311}, for the *L*, *N*, and *T* directions in the section at *X*=52 mm, parallel to the welding line and at different plate depths. ~~Dotted line represents the d_{311} value of the comb also at *X*=52 mm (error is of about ±0.0007 Å).~~QUITÉ COMB

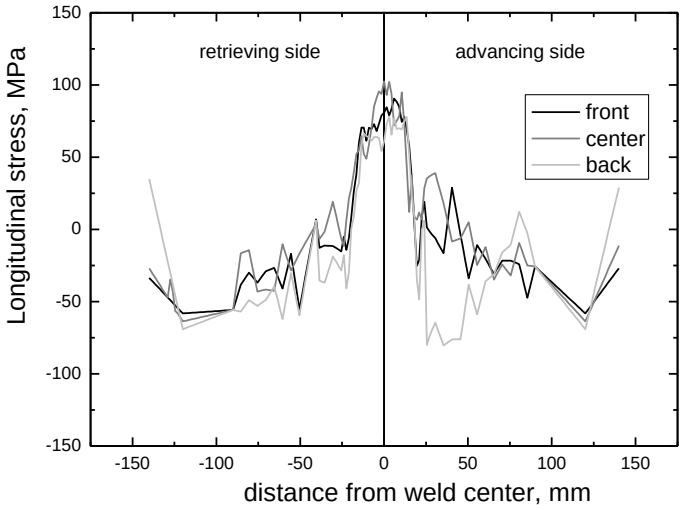
retrieving side
advancing side
front
center
back
Longitudinal stress, MPa
distance from weld center, mm
150
100
50
0
-50
-100
-150

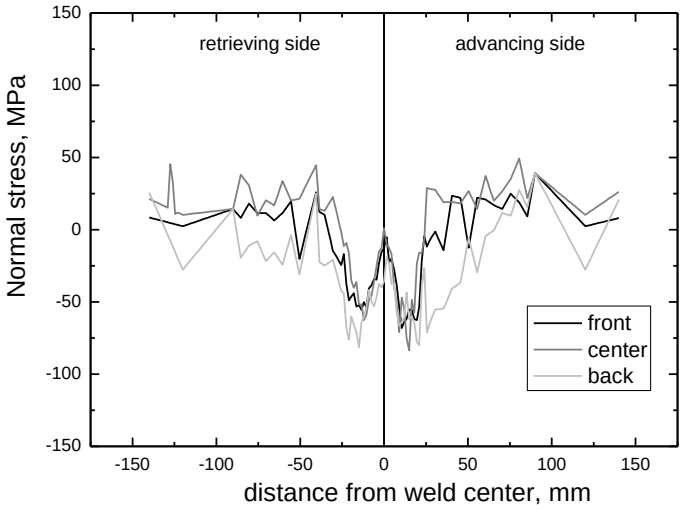
retrieving side
advancing side
front
center
back
Normal stress, MPa
distance from weld center, mm
150
100
50
0
-50
-100
-150

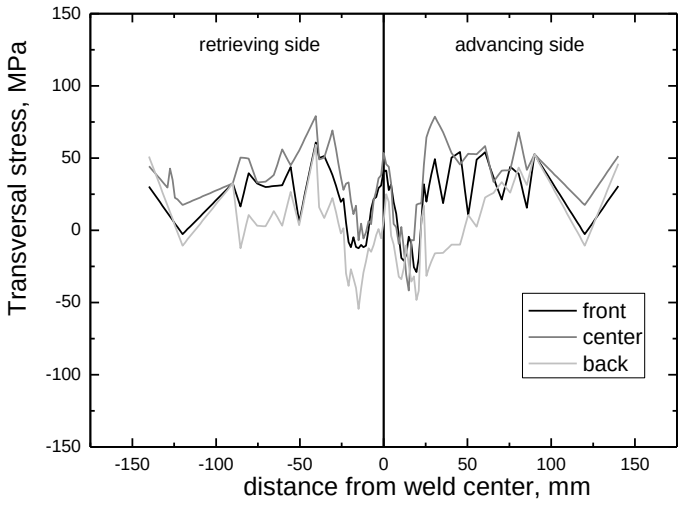
retrieving side
advancing side
front
center
back
Transversal stress, MPa
distance from weld center, mm
150
100
50
0
-50
-100
-150

Figure 7.- Residual stress profiles, *L*, *N*, and *T* components, across the weld calculated with a constant d_0 value obtained from the equilibrium conditions in the longitudinal sections of the plate, at *X*=52 mm and *X*=120 mm (maximum error is of about ±10 MPa).

REHACER CON EL MÓDULO CORRECTO

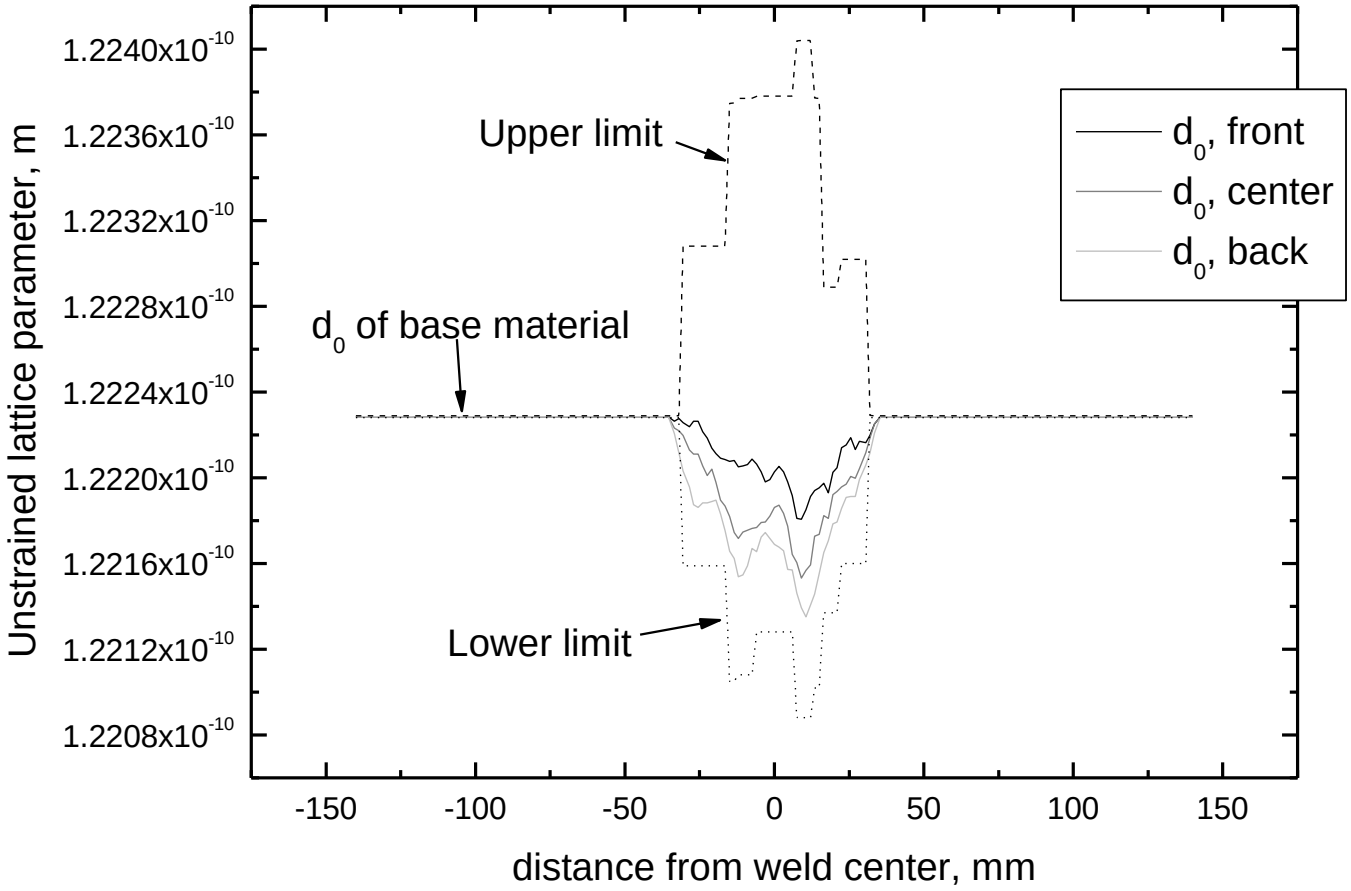

Figure 8.- Profiles of the un-stressed d_0 values (front, center, and back regions) calculated from the equilibrium condition of the longitudinal component on the transverse section of the weld using the GA. The upper and lower d_{311} values used by the GA are included.

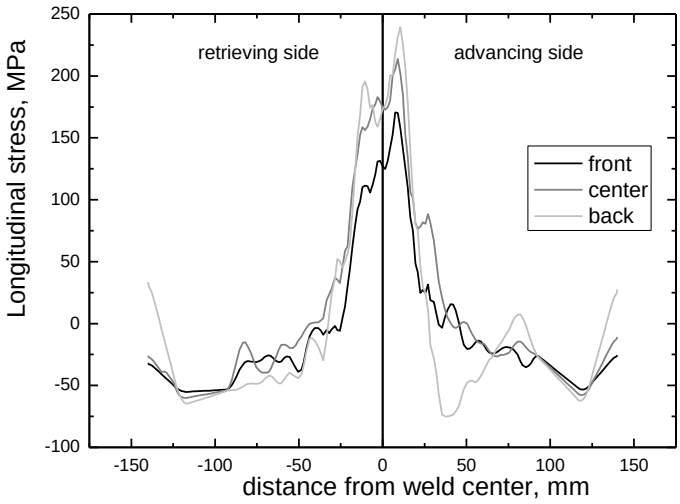
retrieving side
advancing side
front
center
back
Longitudinal stress, MPa
distance from weld center, mm

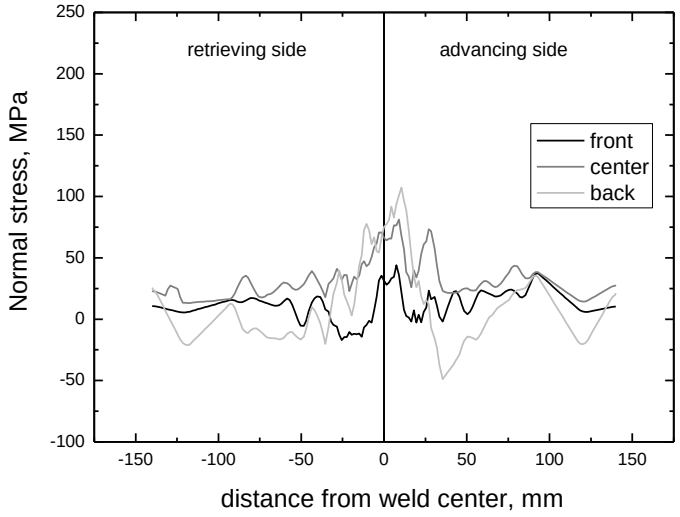
retrieving side
advancing side
front
center
back
Normal stress, MPa
distance from weld center, mm

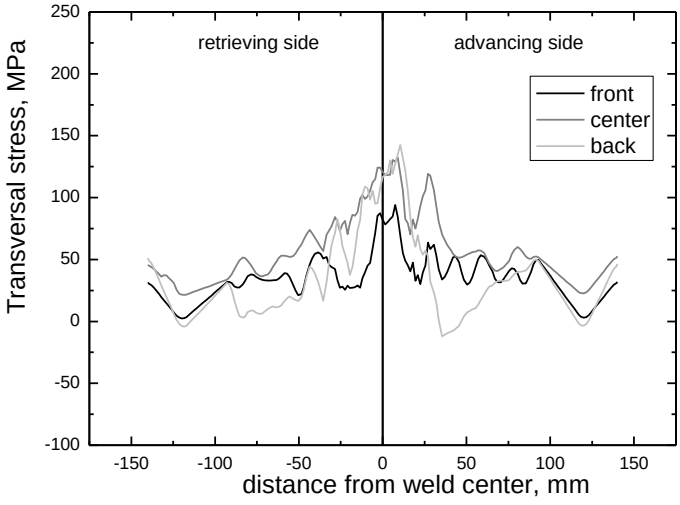
retrieving side
advancing side
front
center
back
Transversal stress, MPa
distance from weld center, mm

Figure 9.- Residual stress profiles across the weld calculated from the un-stressed d_0 values resulting from the GA (data of Fig. 8). CON MODULO CORRECTO

Figure captions

Figure 1.- a) Scheme of the welded plate showing the location on which the RS state was studied and the two longitudinal sections on which d_{311} measurements where conducted. Directions *T*, *L*, and *N* of the reference system coincide with axes *X*, *Y*, and *Z*, respectively. b) Comb sample machined across the weld of the second plate (close to the same region where the RS state was studied in the first plate).

Figure 2.- a) Experimental set-up of SALSA instruments showing the AA7075 welded plate mounted on the hexapod and b) the welded plate used for RS determination. The welding line is parallel to the rolling direction.

Figure 3.- a) Transverse metallograpical section of the weld showing the microstructure developed in the different regions. b) Texture of the as-received AA7075 plate represented as inverse pole figures for the *N* direction at the center and outer regions.

Figure 4.- Inter-planar distance data, d_{311}, as a function of distance from the center of the weld, at the three different depths; front, center, and back, for the three directions *L*, *N*, and *T*. For comparison, the data obtained from the comb sample is also included (error is of about ±0.0007 Å).

Figure 5. Inter-planar distance data, d_{311}, for the *L*, *N*, and *T* directions in the section at *X*=52 mm, parallel to the welding line and at different plate depths. Dotted line represents the d_{311} value of the comb also at *X*=52 mm (error is of about ±0.0007 Å).

~~Figure 6.- Inter planar distance data, d_{311}, for the *L*, *N*, and *T* directions in the comb sample as a function of the distance from the weld center (error is of about ±0.0007 Å).~~

Figure 7.- Residual stress profiles, *L*, *N*, and *T* components, across the weld calculated with a constant d_0 value obtained from the equilibrium conditions in the longitudinal sections of the plate, at *X*=52 mm and *X*=120 mm (maximum error is of about ±10 MPa).

Figure 8.- Profiles of the un-stressed d_0 values (front, center, and bottom regions) calculated from the equilibrium condition of the longitudinal component on the transverse section of the weld using the GA. The upper and lower d_{311} values used by the GA are included.

Figure 9.- Residual stress profiles across the weld calculated using the un-stressed d_0 values resulting from the GA (data of Fig. 8).

References

1.- J. Altenkirch, M. J Peel, A. Steuwer, and P. J Withers, “Comparison of methods to determine variations in unstrained unit cell parameter across welds” J. of Strain Analysis for Engineering Design, vol.46 (2011) pp. 651-662.

2.- S. Ganguly, L. Edwards, and M.E. Fitzpatrick “Problems in using a comb sample as a stress-free reference for the determination of welding residual stress by diffraction” Materials Science and Engineering A, vol. 528 (2011) pp. 1226–1232.

3.- D.J. Hughes, M.N. James, D.G. Hattingh, and P.J. Webster, “The use of combs for evaluation of strain-free references for residual strain measurements by neutron and synchrotron x-ray diffraction” Journal of Neutron Research, vol. 11(4) (2003) pp. 289-293.

4.- M. B. Prime, T. Gnäupel-Herold, J. A. Baumann, R. J. Lederich, D. M. Bowden, and R. J. Sebring, “Residual stress measurements in a thick, dissimilar aluminum alloy friction stir weld” Acta Mater. Vol. 54 -15 (2006) pp. 4013-4021.

5.- A. Steuwer, M. Dumont, M. Peel, M. Preuss, and P.J. Withers “The variation of the unstrained lattice parameter in an AA7010 friction stir weld” Acta Materialia, vol. 55 (2007) pp. 4111–4120.

6.- J. Altenkirch, A. Steuwer, M. Peel, D.G. Richards, and P.J. Withers “The effect of tensioning and sectioning on residual stresses in aluminium AA7749 friction stir welds” Materials Science and Engineering A, vol. 488 (2008) pp. 16–24.

7.- H. Lombard, D.G. Hattingh, A. Steuwer, and M.N. James “Effect of process parameters on the residual stresses in AA5083-H321 friction stir welds” Materials Science and Engineering A, vol. 501 (2009) pp. 119–124.

8.- R.S. Florea, C.R. Hubbard, K.N. Solanki, D.J. Bammann, W.R. Whittington, and E.B. Marin, “Quantifying residual stresses in resistance spot welding of 6061-T6 aluminum alloy sheets via neutron diffraction measurements”, Jour. Mat. Proc. Tech., vol. 212 (2012) pp. 2358– 2370.

9.- S. Pratihar, V. Stelmukh, M.T. Hutchings, M.E. Fitzpatrick, U. Stuhr, and L. Edwards, “Measurement of the residual stress field in MIG-welded Al-2024 and Al-7150 aluminium alloy compact tension specimens”, Mater. Sci. and Eng. A 437 (2006) 46–53.

10.- W. Woo, V. Em, C. R. Hubbard, H. Lee, and K. S. Park, “Residual stress determination in a dissimilar weld overlay pipe by neutron diffraction”, Mater. Sci. and Eng. A, 528 (2011) 8021– 8027.

11 .- M. A. Sutton, A. P. Reynolds, D.-Q. Wang, and C. R. Hubbard “A Study of Residual Stresses and Microstructure in 2024-T3 Aluminum Friction Stir Butt Welds” Journal of Engineering Materials and Technology, vol. 124 (2002) pp. 215-221.

12.- R.S. Mishra, and Z.Y. Ma, “Friction stir welding and processing” Materials Science and Engineering R, vol. 50 (2005) pp 1–78.

13.- J.H. Holland “Outline for a logical theory of adaptive systems” JACM vol. 9 (1962) pp. 279-314.

14.- B. Li, J. Lin, and X. Yao “A novel evolutionary algorithm for determining unified creep damage constitutive equations” Int. Journal of Mechanical Sciences, vol. 44 (2002) pp. 987–1002.

15.- T. De Vuyst, L. D' Alvise, A. Simar, B. de Meester, and S. Pierret, “Finite element modeling of friction stir welding of aluminum alloy plates - Inverse analysis using a genetic algorithm” Welding in the world, vol. 49 (2005) pp. 47-55.

16.- M.T. Pérez-Prado, M.C. Cristina, O.A. Ruano, and G. González-Doncel “Grain boundary sliding and crystallographic slip during superplasticity of Al–5%Ca–5%Zn as studied by texture analysis” Materials Science and Engineering A, vol. 244 (1998) pp. 216–223.

17.- G. Bruno, T. Pirling, P.J. Withers, W. Hutta, and S. Rowe “SALSA: Strain Analyser for Large and Small Scale Engineering Applications” Journal of Neutron Research, vol. 11 (2003) pp. 235-239.

18.- M.N. James, P.J. Webster, D.J. Hughes, Z. Chen, N. Ratel, S.-P. Ting, G. Bruno, and A. Steuwer "Correlating weld process conditions, residual strain and stress, microstructure and mechanical properties for high strength steel—the role of neutron diffraction strain scanning" Materials Science and Engineering A, vol. 427 (2006) pp. 16–26.

19.- G. Bruno, R. Fernández, and G. González-Doncel "Relaxation of the residual stress in 6061Al-15 vol.% SiCw composites by isothermal annealing" Materials Science and Engineering A, vol. 382 (2004) pp. 188–197.

20.- Metals Handbook, vol.II, 10th Ed. Properties and selection; Nonferrous Alloys and Special-Purpose Materials. 1990, pg. 275.

21.- C.G. Rhodes, W. M. Mahoney, W. H. Bingel, R. A. Spurling, and C. C. Bampton, "Effects of frictions stir welding on microstructure of 7075 aluminum", Scripta Mater. Vol. 36 (1997) pp. 69-75.

22.- C. B. Fuller, M. W. Mahoney, M. Calabrese, and L. Micona, "Evolution of microstructure and mechanical properties in naturally aged 7050 and 7075 Al friction stir welds", Materials Science and Engineering A, vol. 527 (2010) pp. 2233-2240.

23.- M.T. Peréz-Prado, M.C. Cristina, M. Torralba, O.A. Ruano, and G. González-Doncel "Texture gradient evolution in Al-5%Ca-5%Zn sheet alloy after tensile deformation at high superplastic strain rate" Scripta Materialia, Vol. 35 (1996) pp. 1455-1460.

24.- M. Peel, A. Steuwer, M. Preuss, and P.J. Withers "Microstructure, mechanical properties and residual stresses as a function of welding speed in aluminium AA5083 friction stir welds" Acta Materialia, vol. 51 (2003) pp. 4791–4801.

25.- W. Woo, Z. Feng, X.-L. Wang, and S. A. David "Neutron diffraction measurements of residual stresses in friction stir welding: a review", Sci. Technol. Weld. Join., vol. 16 (2011) pp. 23-32.

26.- C. Dalle Donne, E. Lima, J. Wegener, A. Pyzalla, T. Buslaps "Investigations on Residual Stresses in Friction Stir Welds", Proc. 3rd Int. Symp. On 'Friction Stir Welding', Kobe, Japan, September 2001, TWI Ltd.

27.- R. Fernández, G. González-Doncel "Creep behavior of ingot and powder metallurgy 6061Al" Journal of Alloys and Compounds, vol. 440 (2007) pp. 158–167.

28.- V.M. Linton, and M.I. Ripley "Influence of time on residual stresses in friction stir welds in agehardenable 7xxx aluminium alloys" Acta Materialia, vol. 56 (2008) pp. 4319–4327.

29.- S. Ganguly, M.E. Fitzpatrick, and L. Edwards "Use of Neutron and Synchrotron X-Ray Diffraction for Evaluation of Residual Stresses in a 2024-T351 Aluminum Alloy Variable-Polarity Plasma-Arc Weld"

30.- J. Hirch, K. Lücke "Mechanism of deformation and development of rolling textures in polycrystalline f.c.c. metals—I. Description of rolling texture development in homogeneous CuZn alloys" vol.36 (1988) pp. 2863–2882.

31.- I.C. Noyan, J.B. Cohen "Residual Stress; Measurements by Diffraction and Interpretation" Springer Verlag, New York, 1987, p. 51.

32.- P. J. Withers, M. Preuss, A. Steuwer, and J. W. L. Pang "Methods for obtaining the strain-free lattice parameter when using diffraction to determine residual stress" Journal of Applied Crystallography, vol.40 (2007) pp. 891–904.

33 .- S. Ferreira-Barragáns, R. Fernández, P. Fernández-Castrillo, G. González-Doncel "Kinetics of tri-axial and spatial residual stress relaxation: Study by synchrotron radiation diffraction in a 2014Al alloy" Journal of Alloys and Compounds, vol. 523 (2012) pp. 94–101.

34.- A.P. Reynolds, Wei Tang, T. Gnaupel-Herold, H. Prask "Structure, properties, and residual stress of 304L stainlesssteel friction stir welds" Scripta Materialia 48 (2003) 1289–1294.

35.- K, Masubuchi: 'Analysis of welded structures: Residual stresses, distortion, and their consequences', Pergamon Press, USA, 1980.

36.- O. Hatamleh, I. V. Rivero, A. Maredia “Residual Stresses in Friction-Stir-Welded 2195 and 7075 Aluminum Alloys” Metall. Mater. Trans. A, vol. 39 (2008) pp. 2867-2874.

37.- G. Buffa, L. Fratini, S. Pasta, “Residual stresses in friction stir welding: numerical simulation and experimental verification”, invited paper at ICRS-8 8th International Conference on Residual Stresses, Denver Marriott Tech Center Hotel, Denver, Colorado, USA, August 2008.